



Missouri University of Science and Technology  
Scholars' Mine

International Conferences on Recent Advances  
in Geotechnical Earthquake Engineering and  
Soil Dynamics

1991 - Second International Conference on  
Recent Advances in Geotechnical Earthquake  
Engineering & Soil Dynamics

14 Mar 1991, 2:00 pm - 3:30 pm

## Response of Earth Dams in Canyons Subjected to Asynchronous Base Excitation

Panos Dakoulas  
*Rice University, Houston, Texas*

Humayun Hashmi  
*Rice University, Houston, Texas*

Follow this and additional works at: <https://scholarsmine.mst.edu/icrageesd>

 Part of the [Geotechnical Engineering Commons](#)

### Recommended Citation

Dakoulas, Panos and Hashmi, Humayun, "Response of Earth Dams in Canyons Subjected to Asynchronous Base Excitation" (1991). *International Conferences on Recent Advances in Geotechnical Earthquake Engineering and Soil Dynamics*. 23.

<https://scholarsmine.mst.edu/icrageesd/02icrageesd/session07/23>

This Article - Conference proceedings is brought to you for free and open access by Scholars' Mine. It has been accepted for inclusion in International Conferences on Recent Advances in Geotechnical Earthquake Engineering and Soil Dynamics by an authorized administrator of Scholars' Mine. This work is protected by U. S. Copyright Law. Unauthorized use including reproduction for redistribution requires the permission of the copyright holder. For more information, please contact [scholarsmine@mst.edu](mailto:scholarsmine@mst.edu).



# Response of Earth Dams in Canyons Subjected to Asynchronous Base Excitation

**Panos Dakoulas**  
Assistant Professor, Department of Civil Engineering, Rice  
University, Houston, Texas

**Humayun Hashmi**  
Graduate Student

**SYNOPSIS:** A mathematical solution is presented for steady-state lateral response of earth and rockfill dams in canyons subjected to asynchronous excitation consisting of obliquely incident SH waves. The dam is idealized with a 2-dimensional shear wedge and the canyon is considered rectangular and consisting of flexible rock. A parametric study is undertaken to investigate the influence of (a) the angle of incidence, (b) the impedance ratio and (c) the canyon narrowness on the steady-state response, by considering in a simplifying way the effects of the dam-canyon interaction.

The results demonstrate that the above factors may have a significant effect on the lateral response of the dam. For relatively flexible canyon rock, the effect of radiation damping is very important and, consequently, the assumption of rigid base may be very unrealistic. Due to interference phenomena, the response is not maximum for vertically propagating waves, but for waves incident at a certain angle. For obliquely incident waves travelling from left to the right, a gradual shift of the location of the peak response is observed from the mid-crest to the right side of the dam as the angle of incidence increases. Also, for very long dams subjected to high frequency obliquely incident waves, there is no amplification of the motion by the dam and, at a certain frequency of excitation, the presence of standing waves is indicated.

## INTRODUCTION

Earthquakes can pose a serious threat to the safety of earth and rockfill dams and cause extensive life loss and property damage. In the last decade significant progress has been made in understanding the dynamic characteristics and seismic behavior of earth and rockfill dams and new analytical models have been developed for the evaluation of their response during strong earthquakes (Martinez and Bielak, 1980; Ohmachi, 1981; Makdisi et al, 1982; Gazetas, 1982; Abdel-Ghaffar et al, 1982; Mejia et al, 1982 and 1983; Dakoulas and Gazetas, 1985, 1986 and 1987; Dakoulas, 1990). A comprehensive review on recent developments was given by Gazetas (1987). Despite this significant progress, a number of potentially quite important aspects of the seismic behavior of dams are yet to be fully understood. The effect of the spatial variation of the earthquake excitation along the dam-canyon interface is one of them.

Seismic waves travelling through different paths with varying material and geometric characteristics are already incoherent, when they arrive at the dam site. This incoherence may be more pronounced in the case of a dam close to an extended earthquake source, where waves may originate from different locations. Moreover, local geological characteristics may force the propagating waves into a series of reflections and refractions, resulting in motions which may be longer than the original earthquake motion, may have new frequency and amplitude characteristics and attack the dam at various angles. It is expected that, in general, due to destructive interference caused by the spatial variability of the excitation, the overall response of such a dam will tend to be smaller than the response of a dam subjected to synchronous excitation (such as the excitation enforced by the rigid canyon assumption).

The effects of a spatial variability of ground excitation may be studied either with a simplified deterministic approach, in which the excitation may be idealized with a steady train of SH waves propagating at an arbitrary angle  $\theta$  to the vertical, or with a stochastic approach, which is more suited for describing the random nature of the spatial variation, but it is mathematically more involved. The present study concentrates on the deterministic approach.

Even in its simplified deterministic form, the problem of a dam in a rectangular canyon subjected to inclined SH waves is a complex boundary value problem. This is because the amplitude and phase of the reflected waves are unknown and vary along the dam-canyon interfaces.

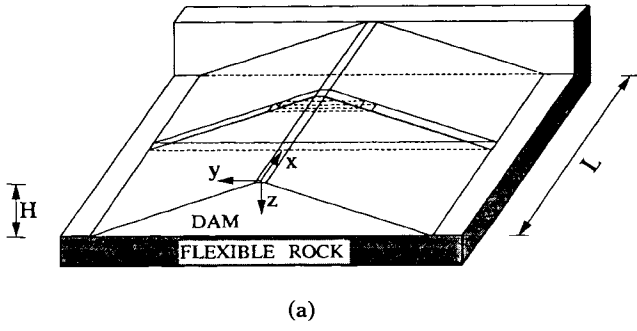
Also, for inclined waves propagating from the left to the right, the right vertical boundary is in a "shadow" with respect to the directly incident waves, but it is attacked by waves transmitted through the dam. Consequently, the evaluation of the total motion along the entire dam-canyon interface must be computed as part of the solution by considering the dam-canyon interaction. The objective of this study is to investigate the effect of the spatial variation of the ground excitation combined with the influence of the aforementioned factors and provide a better understanding of their importance. Such understanding will assist in improving the design of new dams and in evaluating more realistically the safety of thousands of earthfill and rockfill dams built in seismic regions. Moreover, it could assist in interpreting the spatial variation of recorded motions, which may be impossible to explain using models that assume a synchronous base excitation. Although there is no similar study known to the authors addressing this problem, some aspects of the problem have been studied by researchers investigating the response of soil layers and alluvial deposits in canyons (Trifunac, 1973, 1977; Wong and Trifunac, 1974; Roesset, 1977; Aki, 1988).

In this study, the 3-dimensional dam structure is assumed to respond mainly in shear and thus, it may be idealized with a 2-dimensional shear wedge, while the canyon is assumed rectangular and consisting of flexible rock.

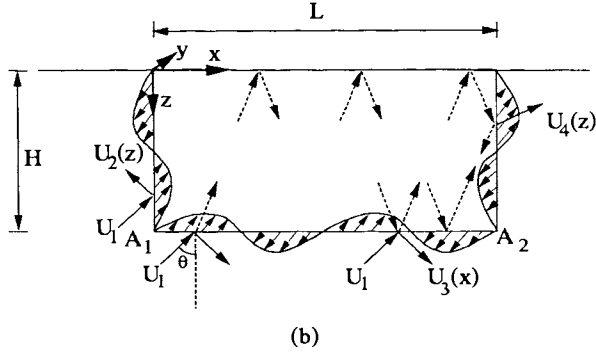
## THE MODEL

Figure 1a portrays a perspective view of the geometry of the dam in a rectangular canyon. Although the canyon shape is idealized as a rectangle solely for mathematical convenience, in many actual canyons an equivalent rectangle offers a reasonable approximation. The dam has a triangular cross-section and consists of a uniform and linearly hysteretic soil with mass density,  $\rho_s$ , shear modulus,  $G_s$ , and hysteretic damping ratio,  $\beta_s$ . Similarly, the canyon consists of a uniform and linearly hysteretic rock with mass density,  $\rho_r$ , shear modulus,  $G_r$ , and hysteretic damping,  $\beta_r$ .

The incident excitation consists exclusively of steady-state harmonic SH waves of a constant amplitude,  $U_1$ , and a frequency,  $\omega$ , travelling from



(a)



(b)

Figure 1.(a) Perspective View of Dam Geometry; (b) Incident, Reflected and Transmitted Waves at the Dam -Canyon Interfaces.

the left to the right along the dam in a upward direction forming an angle  $\theta$  to the vertical (see Fig. 1b). Its displacement,  $u_1$ , is only in the upstream-downstream ( or  $y$  ) direction and has the form

$$u_1 = U_1 e^{i\omega \left( t - \frac{x}{V_x} + \frac{z}{V_z} \right)} \quad (1)$$

in which  $V_x$  and  $V_z$  are the phase velocities along the  $x$  and  $z$  directions given by

$$V_x = \frac{V_r}{\sin \theta} \quad (2)$$

and

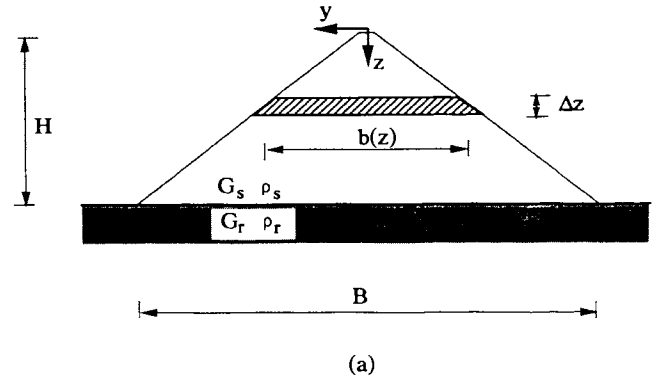
$$V_z = \frac{V_r}{\cos \theta} \quad (3)$$

The unknown displacement,  $u_{1b} = u_{1b}(z)$ , along the left vertical boundary is the summation of the incident and reflected waves and may be written as

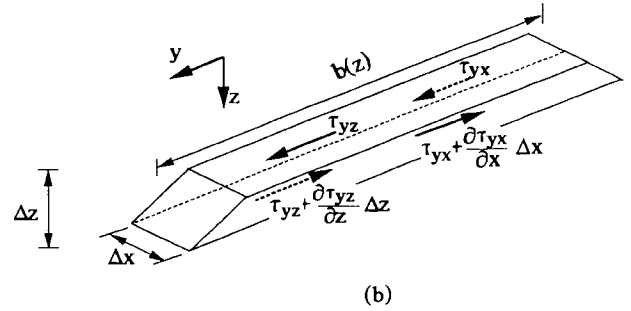
$$u_{1b} = U_1 e^{i\omega \left( t + \frac{z}{V_z} \right)} + U_2 e^{i\omega \left( t + \frac{z}{V_z} \right)} = U_{1b} e^{i\omega t} \quad (4)$$

where  $U_2 = U_2(z)$  and  $U_{1b} = U_{1b}(z)$  are the amplitudes of the reflected and total motion, respectively. It should be noted that  $U_2$  is a complex number and therefore a phase difference may exist between the incident and reflected wave. In fact the term amplitude is exact only for the incident wave,  $U_1$ , while for the reflected waves and the response within the dam the term is used only in a relative sense. This particular form for the motion is adopted only for mathematical convenience and without any loss of generality.

Similarly, the unknown displacement,  $u_b$ , at the dam base is



(a)



(b)

Figure 2.(a) Dam Cross-Section and (b) Infinitesimal Element with Shear Stresses acting at its faces.

$$u_b = U_1 e^{i\omega \left( t - \frac{x}{V_x} + \frac{H}{V_z} \right)} + U_3 e^{i\omega \left( t - \frac{x}{V_x} - \frac{H}{V_z} \right)} = U_b e^{i\omega t} \quad (5)$$

in which  $U_3 = U_3(x)$  and  $U_b = U_b(x)$  are the displacement amplitudes of the reflected and total motion at the base, respectively. The right vertical boundary is in "shadow" with respect to the incident SH waves. Nevertheless, it is subjected to harmonic motion,  $u_{rb} = u_{rb}(z)$ , due to the response of the right side of the canyon to its base excitation and to the waves which propagate through the dam reflecting on and transmitting through this boundary. The unknown displacement  $u_{rb}$  is written as

$$u_{rb} = U_4 e^{i\omega \left( t - \frac{L}{V_x} \right)} = U_{rb} e^{i\omega t} \quad (6)$$

where  $U_{rb} = U_{rb}(z)$  is the amplitude of the total motion along the vertical boundary. Consequently, the total excitation along the three interfaces varies from point to point in both amplitude and phase and will be determined as part of the solution of the problem by considering the dam-canyon interaction. It should be noted that the above is an idealization representing an approximation of the actual transmission and reflection of inclined harmonic SH waves. In reality, the presence of vertical boundaries of the canyon induces some additional reflections along the surface of the half space near the canyon. The effect of these additional reflections is considered secondary and is neglected in this model for mathematical simplicity.

The response of the dam to the above asynchronous excitation applied along its three boundaries is assumed to be only in horizontal lateral shear deformation with the upstream-downstream displacements,  $u$ , uniformly distributed across the width of the dam. In other words, the dam is idealized as a "shear beam", which extends in the vertical and longitudinal directions and assumes either uniform or average response values for the upstream-downstream direction. Indeed, the uniformity of displacements,  $u$ , across the width of the dam has been confirmed by a series of seismic analyses of the earth dams represented with consistent finite-element and shear beam models (Dakoulas and Gazetas,

1985a, 1986b). Fig. 2b shows an infinitesimal element  $b\Delta x\Delta z$  and the corresponding average (across the width  $b$ ) shear stresses  $\tau_{yz}$  and  $\tau_{yx}$  applied on the horizontal and vertical sides, respectively. In reality, the distributions of the  $\tau_{yz}$  and  $\tau_{yx}$  are almost uniform for most of the width  $b$ , except near the two slopes of the dam where the shear modulus is less due to the smaller confining pressure. Nevertheless, by considering the average shear stresses and the average shear modulus across the width, no assumption regarding their exact distribution is required.

The response of the dam to longitudinal and vertical ground motion may be considered independently using similarly simplified beam models. Although only lateral horizontal base motion is considered in this study, some longitudinal and vertical response would indeed take place, but being much less than the lateral response, it is neglected. Finally, hydrodynamic effects are not taken into account, because they are of little importance for the lateral response of the earth dams.

### Steady-State Response

By considering the dynamic equilibrium of an infinitesimal soil element of the dam shown in Fig. 2 and the stress-strain relationships, the equation of motion may be written as

$$G_s^* \left( \frac{\partial^2 u_t}{\partial x^2} + \frac{1}{z} \frac{\partial u_t}{\partial z} + \frac{\partial^2 u_t}{\partial z^2} \right) = \rho_s \ddot{u}_t \quad (12)$$

where  $u_t = u_t(x, z, t)$  is the lateral total displacement and  $G_s^* = G_s(1 + 2i\beta_s)$ , in which  $G_s$  is the shear modulus of soil,  $\beta_s$  is the linear hysteretic damping of soil and  $i = \sqrt{-1}$ . For harmonic steady-state vibration of frequency  $\omega$ , the total displacement,  $u_t$ , in the dam may be written as

$$u_t(x, z, t) = u(x, z, t) + u_b(x, z, t) \quad (13)$$

where  $u = U(x, z) e^{i\omega t}$  is the motion of the dam relative to the motion of base and  $u_b = U_b(x, z) e^{i\omega t}$  is the motion at the base rock given in equation (5). Substituting equation (13) and introducing dimensionless variables, equation (12) may be re written as

$$\begin{aligned} \frac{\partial^2 U}{\partial \eta^2} + \frac{1}{\eta} \frac{\partial U}{\partial \eta} + \left( \frac{\pi H}{L} \right)^2 \frac{\partial^2 U}{\partial \xi^2} + \left( \frac{\omega H}{V_s^*} \right)^2 U &= \\ &= - \left( \frac{\omega H}{V_s^*} \right)^2 U_b - \left( \frac{\pi H}{L} \right)^2 \frac{d^2 U_b(\xi)}{d\xi^2} \end{aligned} \quad (14)$$

where

$$\eta = \frac{z}{H} \quad 0 \leq \eta \leq 1 \quad (15)$$

$$\xi = \frac{x\pi}{L} \quad 0 \leq \xi \leq 1 \quad (16)$$

$$V_s^* = \sqrt{\frac{G_s^*}{\rho_s}} \quad (17)$$

The solution of equation (14) must satisfy the boundary condition of zero shear stress  $\tau_{yz}$  at the dam crest ( $\eta = 0$ ), i. e.,

$$\tau_{xz}(\xi, 0, \omega) = G_s^* \frac{\partial u}{\partial \eta} = 0 \quad (18)$$

The continuity of displacements along the dam base and the left and right vertical boundaries yields, respectively, the following conditions: at the dam base ( $\eta = 1$ ),

$$u(\xi, 1) = 0 \quad 0 \leq \xi \leq \pi \quad (19)$$

at left vertical boundary ( $\xi = 0$ ),

$$u(0, \eta) = u_{1b}(\eta) - u_b(0) = U(0, \eta) e^{i\omega t} \quad \text{where}$$

$$U(0, \eta) = U_1 e^{-\left(\frac{i\omega\eta H}{V_z}\right)} + U_2 e^{\left(\frac{i\omega\eta H}{V_z}\right)} - U_1 e^{\left(\frac{i\omega H}{V_z}\right)} - U_3 e^{-\left(\frac{i\omega H}{V_z}\right)} \quad (20)$$

and at the right vertical boundary ( $\xi = \pi$ ),

$$u(\pi, \eta) = u_{rb}(\eta) - u_b(\pi) = U(\pi, \eta) e^{i\omega t} \quad \text{where}$$

$$U(\pi, \eta) = U_4(\eta) e^{-\left(\frac{i\omega L}{V_x}\right)} - U_1 e^{-i\omega\left(\frac{L}{V_x} - \frac{H}{V_z}\right)} - U_3 e^{-i\omega\left(\frac{L}{V_x} + \frac{H}{V_z}\right)} \quad (21)$$

Finally the continuity of shear stresses  $\tau_{yz}$  at the dam base and  $\tau_{yx}$  at the left and right vertical boundaries provides three more equations: at the dam base ( $\eta = 1$ ),

$$\frac{\partial U}{\partial \eta} = \frac{G_r^* i\omega H}{G_s^* V_z} \left( U_1 e^{i\omega H/V_z} - U_3 e^{-i\omega H/V_z} \right) e^{-i\omega \xi L/\pi V_x} \quad (22)$$

at left vertical boundary ( $\xi = 0$ ),

$$\frac{\partial U}{\partial \xi} = \frac{G_r^* i\omega L}{G_s^* \pi V_x} (U_2 - U_1) e^{i\omega \eta H/V_z} - \frac{dU_b(0)}{d\xi} \quad (23)$$

and at the right vertical boundary ( $\xi = \pi$ ),

$$\frac{\partial U}{\partial \xi} = - \frac{G_r^* i\omega L}{G_s^* \pi V_x} U_4 e^{-i\omega L/V_x} - \frac{dU_b(\pi)}{d\xi} \quad (24)$$

By taking Finite-Cosine Transform with respect to  $\xi$ , the equation of motion (14) becomes,

$$\begin{aligned} \frac{d^2 \mathbf{u}}{d\eta^2} + \frac{1}{\eta} \frac{d\mathbf{u}}{d\eta} + \left( \left( \frac{\omega H}{V_s^*} \right)^2 - \left( \frac{n\pi H}{L} \right)^2 \right) \mathbf{u} &+ \left( (-1)^n \frac{\partial U(\xi=\pi)}{\partial \xi} - \frac{\partial U(\xi=0)}{\partial \xi} \right) = \\ &= \left( \left( \frac{n\pi H}{L} \right)^2 - \left( \frac{\omega H}{V_s^*} \right)^2 \right) (\mathbf{u}_1 + \mathbf{u}_3) + \frac{dU_b(\xi=0)}{d\xi} - (-1)^n \frac{dU_b(\xi=\pi)}{d\xi} \end{aligned} \quad (25)$$

where the bold characters denote the Finite-Cosine Transform of  $U$  given by

$$\int_0^\pi U \cos(n\xi) d\xi \quad (26)$$

$$\mathbf{u}_1 = \int_0^\pi U_1 e^{i\omega(H/V_z - \xi L/\pi V_x)} \cos(n\xi) d\xi \quad (27)$$

$$\mathbf{u}_3 = \int_0^\pi U_3 e^{-i\omega(H/V_z + \xi L/\pi V_x)} \cos(n\xi) d\xi \quad (28)$$

Substituting the boundary conditions from equations (23) and (24) and cancelling the common terms, equation (25) yields,

$$\frac{d^2 \mathbf{u}}{d\eta^2} + \frac{1}{\eta} \frac{d\mathbf{u}}{d\eta} + (k^2 - a^2) \mathbf{u} = (a^2 - k^2)(\mathbf{u}_1 + \mathbf{u}_3) + \beta^2 \frac{G_r^* i\omega L}{G_s^* \pi V_x} \left[ (U_2 - U_1) e^{i\omega\eta H/V_z} + (-1)^n U_4 e^{i\omega L V_x} \right] \quad (29)$$

in which,

$$k^2 = \left( \frac{\omega H}{V_s} \right)^2 \quad (30)$$

$$a^2 = \left( \frac{n\pi H}{L} \right)^2 \quad \text{and} \quad (31)$$

$$\beta^2 = \left( \frac{\pi H}{L} \right)^2 \quad (32)$$

Moreover, by taking the Hankel Transform with respect to  $\eta$  and by using the boundary conditions in equations (18) and (19), equation (25) becomes,

$$-\mu_j \tilde{\mathbf{u}}(n, \mu_j) + (k^2 - a^2) \tilde{\mathbf{u}}(n, \mu_j) = \frac{J_1(\mu_j)}{\mu_j} [\mathbf{u}_1 + \mathbf{u}_3] (a^2 - k^2) + \beta^2 \frac{G_r^* i\omega L}{G_s^* \pi V_x} \left[ \tilde{U}_2(\mu_j) - \tilde{U}_1(\mu_j) + (-1)^n \tilde{U}_4(\mu_j) \right] \quad (33)$$

where  $\tilde{\mathbf{u}}(n, \mu_j)$  is the Hankel transform of  $\mathbf{u}$ ,  $J_1(\mu_j)$  is the Bessel function of first kind and order 1, evaluated at the  $\mu_j$  root of the equation  $J_1(\mu_j)=0$ .

$$\tilde{U}_1 = \int_0^1 U_1 e^{i\omega\eta H/V_z} \eta J_0(\mu_j \eta) d\eta \quad (34)$$

$$\tilde{U}_2 = \int_0^1 U_2 e^{i\omega\eta H/V_z} \eta J_0(\mu_j \eta) d\eta \quad (35)$$

$$\tilde{U}_4 = \int_0^1 U_4 e^{-i\omega L V_x} \eta J_0(\mu_j \eta) d\eta \quad (36)$$

Solving for  $\tilde{\mathbf{u}}(n, \mu_j)$  the transformed solution is obtained

$$\tilde{\mathbf{u}}(n, \mu_j) = \frac{1}{(a^2 + \mu_j^2 - k^2)} \cdot \left( (\mathbf{u}_1 + \mathbf{u}_3) (k^2 - a^2) \frac{J_1(\mu_j)}{\mu_j} + \beta^2 \frac{G_r^* i\omega L}{G_s^* \pi V_x} [\tilde{U}_1 - \tilde{U}_2 - (-1)^n \tilde{U}_4] \right) \quad (37)$$

Taking the inverse Hankel Transform of equation (37),

$$\mathbf{u} = 2 \sum_{j=1}^{\infty} \frac{\tilde{\mathbf{u}}(n, \mu_j) J_0(\mu_j \eta)}{J_1^2(\mu_j)} \quad (3)$$

Finally taking the inverse Finite-Cosine Transform yields,

$$U = 2 \sum_{j=1}^{\infty} \left( \frac{\tilde{\mathbf{u}}(0, \mu_j) J_0(\mu_j \eta)}{\pi J_1^2(\mu_j)} + \frac{2}{\pi} \sum_{n=1}^{+\infty} \frac{\tilde{\mathbf{u}}(n, \mu_j) J_0(\mu_j \eta) \cos(n\xi)}{J_1^2(\mu_j)} \right) \quad (3)$$

Note that  $\tilde{\mathbf{u}}(n, \mu_j)$  involves three unknowns, namely,  $\mathbf{u}_3$ ,  $\tilde{U}_3$ ,  $\tilde{U}_4$ , which can be found by using the remaining three boundary conditions. Enforcing the boundary condition in equation (20),

$$(U_1 + U_2) e^{i\omega\eta H/V_z} - (U_1 e^{i\omega H/V_z} + U_3(\xi=0) e^{-i\omega H/V_z}) = 2 \sum_{j=1}^{\infty} \left( \frac{\tilde{\mathbf{u}}(0, \mu_j) J_0(\mu_j \eta)}{\pi J_1^2(\mu_j)} + \frac{2}{\pi} \sum_{n=1}^{+\infty} \frac{\tilde{\mathbf{u}}(n, \mu_j) J_0(\mu_j \eta)}{J_1^2(\mu_j)} \right) \quad (40)$$

and taking the Hankel Transform of equation (40) with respect to leads to

$$\tilde{U}_1 + \tilde{U}_2 - (U_1 e^{i\omega H/V_z} + U_3(\xi=0) e^{-i\omega H/V_z}) \frac{J_1(\mu_j)}{\mu_j} = \frac{\tilde{\mathbf{u}}(0, \mu_j)}{\pi} + \frac{2}{\pi} \sum_{n=1}^{+\infty} \tilde{\mathbf{u}}(n, \mu_j) \quad (41)$$

Similarly, enforcing the boundary condition in equation (21)

$$\left[ U_4 - (U_1 e^{i\omega H/V_z} + U_3(\xi=\pi) e^{-i\omega H/V_z}) \right] e^{-i\omega L V_x} = 2 \sum_{j=1}^{\infty} \left( \frac{\tilde{\mathbf{u}}(0, \mu_j) J_0(\mu_j \eta)}{\pi J_1^2(\mu_j)} + \frac{2}{\pi} \sum_{n=1}^{+\infty} \frac{\tilde{\mathbf{u}}(n, \mu_j) J_0(\mu_j \eta) \cos(n\pi)}{J_1^2(\mu_j)} \right) \quad (42)$$

and taking the Hankel Transform of equation (42) with respect to leads to

$$\tilde{U}_4 - (U_1 e^{i\omega H/V_z} + U_3(\xi=\pi) e^{-i\omega H/V_z}) e^{-i\omega L V_x} \frac{J_1(\mu_j)}{\mu_j} = \frac{\tilde{\mathbf{u}}(0, \mu_j)}{\pi} + \frac{2}{\pi} \sum_{n=1}^{+\infty} \tilde{\mathbf{u}}(n, \mu_j) \cos(n\pi) \quad (43)$$

Finally, enforcing the boundary condition in equation (22),

$$\frac{G_r^* i\omega H}{G_s^* V_z} (U_1 e^{i\omega H/V_z} - U_3 e^{-i\omega H/V_z}) e^{-i\omega \xi L/\pi V_x} = 2 \sum_{j=1}^{\infty} \left( \frac{\mu_j \tilde{\mathbf{u}}(0, \mu_j)}{\pi J_1(\mu_j)} + \frac{2}{\pi} \sum_{n=1}^{+\infty} \frac{\mu_j \tilde{\mathbf{u}}(n, \mu_j) \cos(n\xi)}{J_1(\mu_j)} \right) \quad (44)$$

and taking the Finite - Cosine Transform with respect to  $\xi$  one has,

$$\frac{G_r^* i\omega H}{G_s^* V_s} (\mathbf{u}_1 - \mathbf{u}_3) = 2 \sum_{j=1}^{\infty} \frac{\mu_j \tilde{\mathbf{u}}(n, \mu_j)}{J_1(\mu_j)} \quad (45)$$

Equations (41), (43) and (45) can be solved simultaneously to get  $\mathbf{u}_3$ ,  $\tilde{\mathbf{U}}_2$ , and  $\tilde{\mathbf{U}}_4$ , whereas the two other unknowns,  $U_3(\xi=0)$  and  $U_3(\xi=\pi)$  involved in equations (41) and (43) can be found by equating shear stresses,  $\tau_{xy}$ , in the rock and dam at points  $A_1$  and  $A_2$  in Fig. 1b (Hashmi, 1989). Hence, the steady-state solution for total displacements  $u_t = u_t(\eta, \xi, t)$  is given by,

$$u_t = \left[ 2 \sum_{j=1}^{\infty} \left( \frac{\tilde{\mathbf{u}}(0, \mu_j) J_0(\mu_j \eta)}{\pi J_1^2(\mu_j)} + \frac{2}{\pi} \sum_{n=1}^{\infty} \frac{\tilde{\mathbf{u}}(n, \mu_j) J_0(\mu_j \eta) \cos(n\xi)}{J_1^2(\mu_j)} \right) + U_b \right] e^{i\omega t} \quad (46)$$

It is of interest to compute the amplification function, AF, defined as the ratio of the amplitude of the acceleration at any given point within the dam divided by the amplitude of the acceleration at the outcrop rock. For harmonic motion, the acceleration amplification is identical to the absolute displacement amplification and may be computed using equation (46) as

$$AF = U_t / 2U_1 \quad (47)$$

where  $U_t$  is the absolute value of  $u_t$ . Figure 3 illustrates a perspective view of the AF along the dam crest versus a dimensionless frequency  $\omega H / V_s$  for a dam with  $L/H = 3$ ,  $V_r/V_s = 3$ ,  $\beta_s = 0.1$ ,  $\beta_r = 0$  and SH waves incident at  $\theta = 30^\circ$ . Equation (47) is utilized in a series of parametric studies aimed at evaluating the effect of the asynchronous base motion on the response of the dam-canyon system. Some results from these studies are presented in the following.

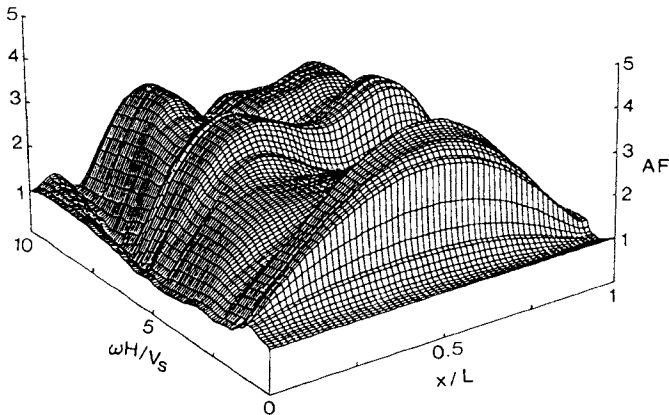


Figure 3. Amplification along the Dam Crest versus a Dimensionless Frequency.

#### PARAMETRIC STUDY AND DISCUSSION

A parametric study is undertaken to investigate the influence of three parameters on the steady-state response of a dam subjected to steady train of propagating SH waves, by considering the effect of dam-canyon interaction. In particular, the study focuses on the effects of: (a) the angle of incidence (b) the impedance ratio (c) the canyon narrowness.

The results are presented in the form of amplification functions (AF) of absolute acceleration. AF is computed with reference to the acceleration of the outcrop rock having an amplitude which is twice the amplitude of the incident waves.

#### Effect of angle of incidence

To investigate the effect of the angle of incidence, a dam is considered with a length to height ratio  $L/H = 3$ , an S-wave velocity ratio  $V_r/V_s = 3$ , a mass density ratio  $\rho_r/\rho_s = 1.5$  and material damping  $\beta_s = 0.1$  and  $\beta_r = 0$  for the soil (s) and the rock (r), respectively. Figure 4 plots the amplification function, AF, evaluated along the length of the dam crest for five values of the angle of incidence  $\theta = 5^\circ, 30^\circ, 45^\circ, 60^\circ$ , and  $75^\circ$ . The frequency of the input excitation is selected equal to the fundamental natural frequency of the dam in the flexible canyon.

The most important observation from Figure 4 is that all response values are considerably less than those of a similar dam built in a rigid canyon, yielding a mid-crest amplification at first resonance slightly above 10. This is mainly due to the presence of the flexible rock canyon base resulting in significant radiation damping of the system. The effect of the spatial variability of the motion, depending on the angle of incidence  $\theta$ , is also important, especially for large values of  $\theta$ . Figure 4 suggests that the latter factor should be considered for a more realistic interpretation of recorded acceleration at existing dams. Notice that the maximum response does not occur for vertical waves, but for waves forming an angle  $\theta \approx 35^\circ$ . This may be explained by the fact that the response depends on the interference of waves transmitted through the base and the vertical abutments: for  $\theta = 0^\circ$  the motion is synchronous at the base and asynchronous at the vertical abutments, but as  $\theta$  increases, the motion becomes more asynchronous at the base and less asynchronous at the left vertical boundary, resulting in a maximum response at  $\theta \approx 35^\circ$ . Also, as expected, the response of the right vertical boundary is less than the response of the left boundary.

Another interesting observation in Figure 4 is the gradual shift of the amplification peaks to the right side of the dam crest, except for  $\theta = 75^\circ$ .

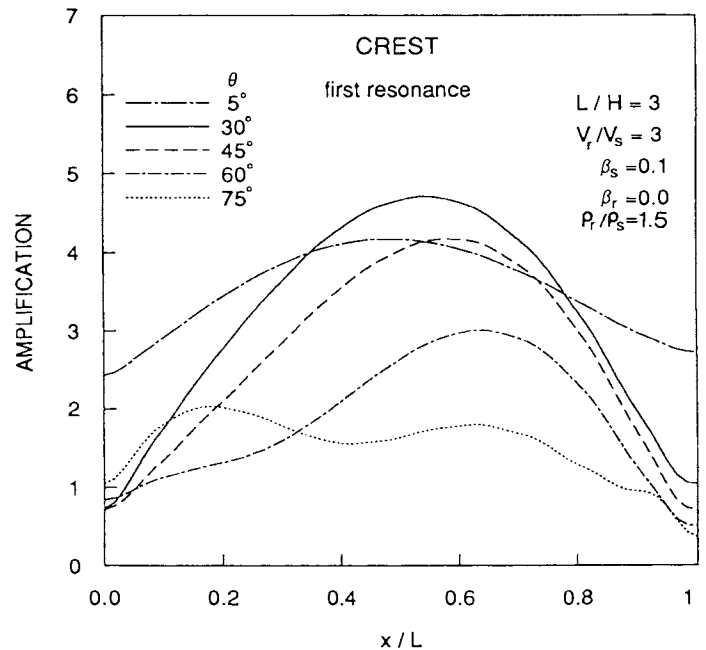


Figure 4. Crest Amplification at the First Natural Frequency of a Dam Subjected to SH waves Incident at  $\theta = 5^\circ, 30^\circ, 45^\circ, 60^\circ$ , and  $75^\circ$ .

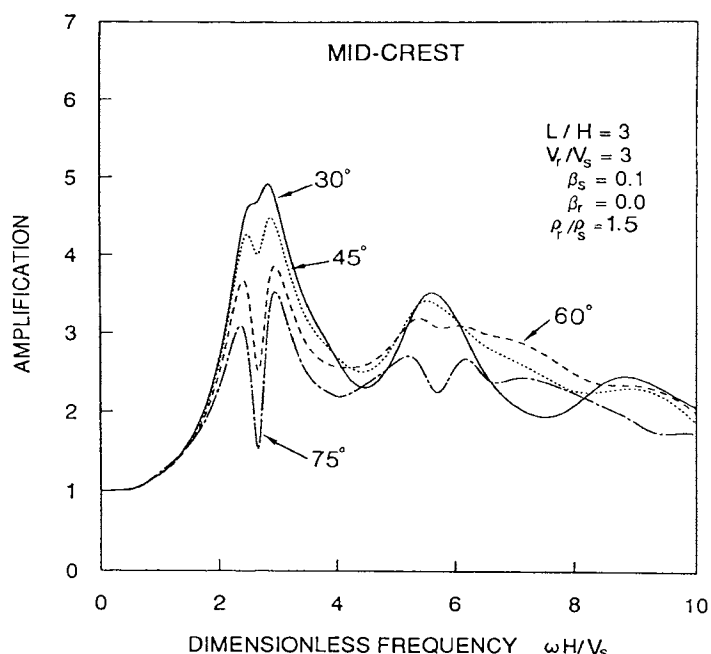
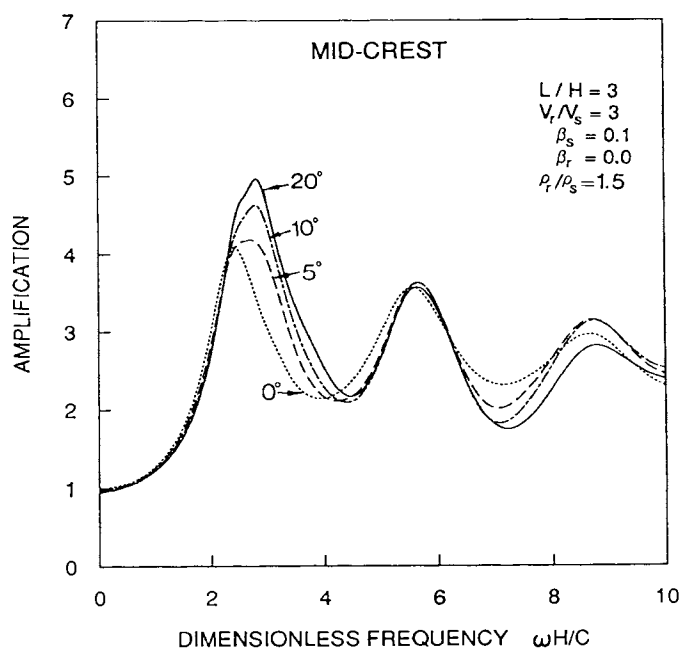


Figure 5. Mid-Crest Amplification versus Dimensionless Frequency of a Dam Subjected to SH Waves at  $\theta$  equal to (a)  $0^\circ$ ,  $5^\circ$ ,  $10^\circ$ ,  $20^\circ$  and (b)  $30^\circ$ ,  $45^\circ$ ,  $60^\circ$ , and  $75^\circ$ .

Of course, for vertical waves the distribution of amplification is symmetric with a peak value at the mid-crest. But as  $\theta$  increases, waves travelling from the left to the right along the dam reflect mostly on the right side of the dam crest and part of them returns to the canyon, while the rest of them continue with a series of reflections within the dam boundaries. For  $\theta \geq 75^\circ$ , the motion at the base becomes more asynchronous while the motion at the left boundary more synchronous and, thus, more important resulting in a stronger response at the left side of the dam. As shown later in this parametric study, the above are true for  $\lambda/L \leq 2$ , where  $\lambda$  is the wavelength of the input motion. For  $\lambda/L \geq 4$ , the dam appears as a small detail in the half space and is practically ignored by the propagating waves. In that case, the dam-canyon system tends to vibrate like a half-space excited by SH waves, showing little variation of response along the crest of the dam.

It is interesting to note that the above results are in complete agreement, in a qualitative manner, with results published by Trifunac (1977, 1973) on the amplification of motion of a semi-cylindrical valley, as well as at the surface of an alluvial deposit in a semi-cylindrical valley, both subjected to incident SH waves at various angles  $\theta$ .

Figure 5 plots the amplification at mid-crest versus a dimensionless frequency  $k = \omega H/V_s$  for various values of  $\theta$ . The variation of the amplification for the entire range of  $\theta$  values is from 3.5 to 5 (for  $V_r/V_s = 3$  and  $L/H = 3$ ).

Figure 6 plots the crest amplification  $AF$  evaluated along the length of the dam for  $\theta = 30^\circ$  and for five ratios of  $\lambda/L = 0.25, 0.5, 1, 2$  and  $4$ , where  $\lambda$  is the wavelength of the incident motion and  $L$  is the dam length. The maximum response is obtained for a frequency  $f = V_r/\lambda$  equal to the first natural frequency of the dam, corresponding to  $\lambda/L = 2$ . Notice that for decreasing  $\lambda/L$  ratios ( $\lambda/L < 2$ ) the high frequency motion at the dam-canyon boundaries excites high-frequency vertical and longitudinal modes of vibration, displaying a larger number of peaks along the dam crest. A very high-frequency input excitation, (i.e.  $\lambda/L = 0.25$ ), causes an overall deamplification of the response at the crest due mainly to a very asynchronous motion at the boundaries. On

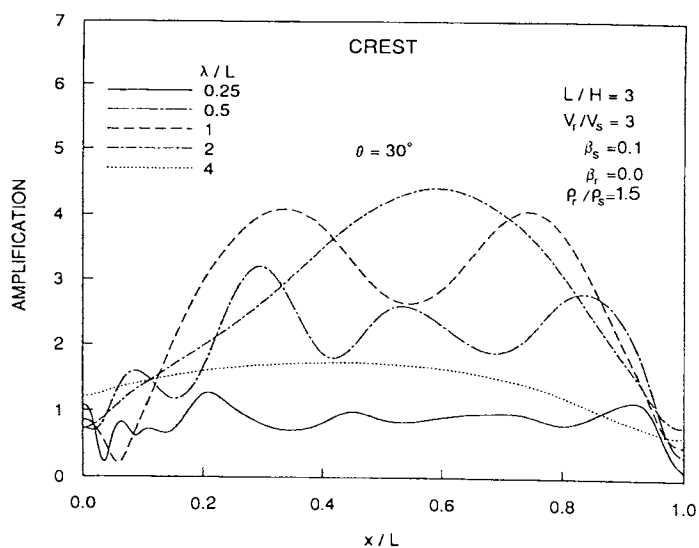


Figure 6. Crest Amplification versus a Dimensionless Frequency for  $\theta = 30^\circ$  and  $\lambda/L = 0.25, 0.5, 1, 2$  and  $4$ .

the other hand, for increasing  $\lambda/L$  ratios ( $\lambda/L > 2$ ) the response decreases again, since large wavelength SH waves hardly "feel" the irregularity caused by the presence of the dam and, therefore, the response of the latter tends to approach the response of the elastic half-space.

#### Effect of the impedance ratio

The impedance ratio is expressed here as the S-wave velocity ratio  $V_r/V_s$ . To investigate the effect of the impedance ratio on the response of

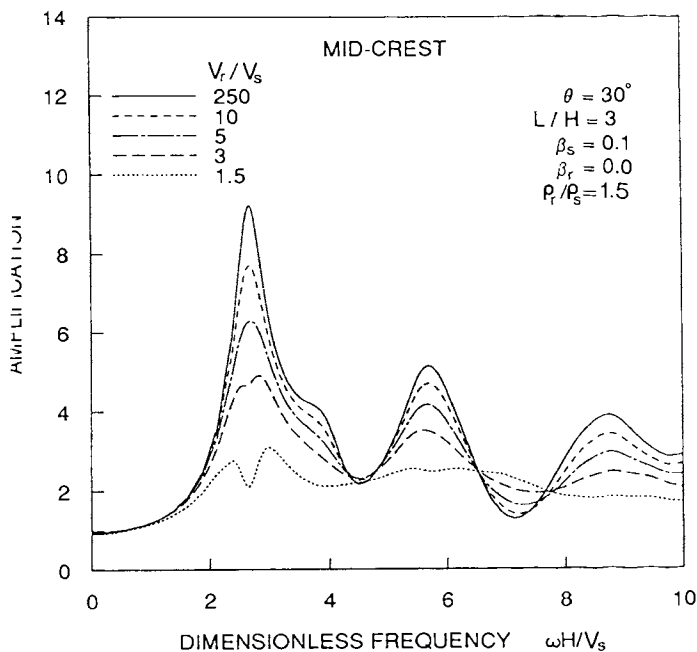


Figure 7. Mid-Crest Amplification versus a Dimensionless Frequency for  $\theta = 30^\circ$ , and  $V_r/V_s = 1.5, 3, 5, 10,$  and  $250$ .

the dam, five dams are considered all having  $L/H = 3$ , mass density ratio  $\rho_r/\rho_s = 1.5$ , material damping  $\beta_s = 0.1$  for the soil and  $\beta_r = 0$  for the canyon rock, and corresponding to five different S-wave velocity ratios  $V_r/V_s = 1.5, 3, 5, 10, 250$ . The angle of incidence  $\theta$  for the SH waves is taken equal to  $30^\circ$ .

The mid-crest amplification functions for the five dams are plotted versus a dimensionless frequency in Fig. 7. The results indicate a dramatic effect of the S-wave velocity ratio on the response. Indeed, the maximum crest amplification varies from about  $AF \approx 3$  for  $V_r/V_s = 1.5$  to  $AF \approx 9.2$  for  $V_r/V_s = 250$ . This suggests that the simplifying assumption of a rigid canyon, which ignores the effect of the radiation damping, may be very misleading.

During an earthquake ground shaking the ratio of  $V_r/V_s$  may increase significantly at severe acceleration pulses, because of the degradation of soil stiffness with increasing shear strain and return to its original value during the weak parts of the excitation. This results to smaller radiation damping during strong acceleration pulses and therefore higher amplification values. By contrast, the hysteretic material damping, which depends also on the level of cyclic shear strain, increases during the strong acceleration pulses resulting into a reduced amplification of the motion. A realistic evaluation of the response of the dam should account for the opposing effects of both the material and radiation damping variation during an earthquake shaking.

A comparison between mid-crest amplification results derived from the flexible canyon solution presented in this study and the independently derived rigid canyon solution showed that, as  $V_r/V_s$  approaches infinity, the flexible canyon solution approaches the that of the rigid canyon. This agreement can also be seen in Figure 6, in which the AF for  $V_r/V_s = 250$  approaches the rigid canyon amplification, which has a peak value about 10.

#### Effect of canyon narrowness

For a given canyon shape, the canyon narrowness may be expressed by using the ratio of the length over the height of the dam,  $L/H$ . To investigate the effect of the canyon narrowness on the response, four dams are considered, all having an S-wave velocity ratio  $V_r/V_s = 3$ , a mass density ratio  $\rho_r/\rho_s = 1.5$ , material damping  $\beta_s = 0.1$  for the soil

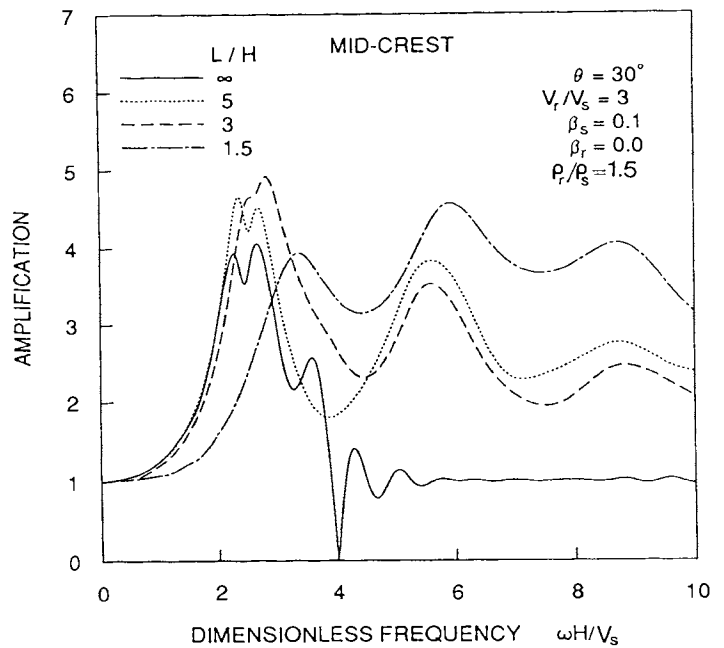


Figure 8. Mid-Crest Amplification versus a Dimensionless Frequency for  $\theta = 30^\circ$  and  $L/h = 1.5, 3, 5,$  and  $\infty$ .

and  $\beta_r = 0$  for the rock, and corresponding to four different values of  $L/H = 1.5, 3, 5$  and  $\infty$ . Again, the angle of incidence  $\theta$  for the SH waves is taken equal to  $30^\circ$ .

The mid-crest amplification functions for the four dams are plotted versus a dimensionless frequency in Figure 8. As expected, increasing canyon narrowness results into higher amplification for the high-frequency part of the spectra in Figure 8. This "stiffening" effect of the canyon narrowness is due to the increasing proximity of the stiffer boundaries of the canyon and is even more pronounced in rigid canyons (Dakoulas and Gazetas, 1987).

Notice for  $L/H = 125$ , there is no crest amplification for  $k = \omega H/V_s$  larger than 5. This is hardly surprising, since, for high frequency excitation, the wave length  $\lambda$  is very small and, therefore, there is significant constructive interference along the very long base of the dam resulting into  $AF=1$ . For lower frequency, however, there is considerable amplification with a peak value  $AF \approx 4$ . Note that peak amplification derived from the plane strain shear beam solution for similar dam on flexible rock, subjected to synchronous base excitation, is also  $AF \approx 4.1$  at first resonance, but the overall amplification spectra of the synchronous and asynchronous analyses are apparently quite different. An interesting feature of the asynchronous amplification curve in Figure 8 is the sharp decay to the a value close to zero for  $\omega H/V_s = 4$ . This may imply standing waves, generated as a result of wave interference, in which the crest becomes a node point, being almost stationary at that frequency. This is also observed by Trifunac (1973) in his study for the response of both a semi-cylindrical alluvial valley and a semi-cylindrical canyon (1977) to SH waves.

#### CONCLUSIONS

This study has developed a new mathematical solution for evaluating the lateral response of earth and rockfill dams in flexible canyons subjected to asynchronous excitation consisting of SH waves incident at an arbitrary angle. The conclusions derived from the presented parametric studies are summarized as follows:



1. The flexibility of the canyon rock has a dramatic effect on the response of the dam, as it affects the amount of energy radiated back to the canyon. The presence of a flexible base rock tends to reduce the amplification peaks at the resonance, particularly at weak excitation in which there is little degradation of soil stiffness. For example, for the dam considered in the parametric study and for vertically propagating waves, the mid-crest amplification, AF, at first resonance is about 10 for rigid canyon rock and about 4 for flexible canyon rock with  $V_r/V_s = 3$ . This clearly demonstrates that the simplifying assumption of a rigid base may be very conservative.

2. For obliquely incident waves travelling from left to the right, as the angle of incidence  $\theta$  increases, the motion tends to become more asynchronous along the base and less asynchronous along the vertical boundary. The response of the dam depends significantly on the interference of the waves transmitted through base and the left vertical boundary. For the cases examined, the maximum response is obtained at an angle  $\theta \approx 35^\circ$  and is about 25% higher than the response caused by vertically propagating waves (which result in a maximum spatial variability of the excitation along the vertical boundary). Moreover, for a large range of  $\theta$ , a gradual shift of the location of the peak response is observed from the mid-crest to the right side of the dam as  $\theta$  increases. The angle of incidence  $\theta$  affects also significantly the variation in amplitude and in phase of the total motion along the base and the two abutments of the dam. (This motion is initially unknown and is computed as part of the solution, by considering the dam-canyon interaction.)

3. For either synchronous or asynchronous excitation, as the canyon narrowness increases, the lateral response of the dam for the high frequency motion increases. In practical terms, this results in higher accelerations and smaller displacements and shear strains within the dam. This is because accelerations depend on many more modes (about 10 or more) compared to displacements and strains which require only about 4. However, for very long dams, high frequency asynchronous excitation results in no amplification of the excitation (AF = 1) while synchronous excitation induces much higher amplification (AF = 2 to 5, for the studied examples). Also, for long dams subjected to asynchronous motion, standing waves are indicated at a dimensionless frequency  $\omega H/V_s = 4$ , as a result of wave interference, in which the crest becomes an almost stationary node point.

4. For low-frequency SH excitation, the response of the dam shows little variation along the crest and approaches the response of the elastic half-space. In this case, the dimensions of the dam are small compared with the wavelength and, therefore, the presence of the dam has only a small effect on the site response.

5. The above results are qualitatively in agreement with results from the response of semi-cylindrical canyons and of alluvial deposits in semi-cylindrical and semi-elliptical canyons subjected to obliquely incident SH waves obtained by Trifunac (1973, 1977). Finally, as the stiffness of the canyon rock increases, the solution of the presented model approaches the independently derived solutions for dams built in rigid canyons. In the latter case, for  $L/H = \infty$ , the presented model approaches the solution for a very long dam on rigid foundation.

## REFERENCES

Abdel-Ghaffar, A. M. & Koh, A.S. (1982) "Three-dimensional Dynamic Analysis of Non-Homogeneous Earth Dams," *Journal of Soil Dynamics and Earthquake Engineering*, 1, 3, pp.136-144.

Aki, K. (1988) "Local Site Effects on Strong Ground Motion", *Proceedings of a Conf. on Earthquake Engineering and Soil Dynamics II; Recent Advances in Ground Motion Evaluation.*, Editor T. L. Von Thun, Park City, Utah.

Dakoulas, P., (1990), "Nonlinear Response of Dams Founded on Alluvial Deposits in Narrow Canyons" *Journal of Soil Dynamics and Earthquake Engineering* (in press).

Dakoulas, P. and Gazetas, G., (1985a) "A Class of Inhomogeneous Shear Models for Seismic Analysis of Dams and Embankments" *Journal of Soil Dynamics and Earthquake Engineering*, Vol. 4, pp. 166-182.

Dakoulas, P. and Gazetas, G. (1985b) "Nonlinear Seismic Response Embankment Dams," *Proceedings of the 2nd International Conference on Soil Dynamics and Earthquake Engineering*.

Dakoulas, P. and Gazetas G. (1986a) "Seismic Shear Vibration Embankment Dams in Semi-Cylindrical Valleys," *Journal of Earthquake Engineering and Structural Dynamics*, Vol.14, pp. 19-40.

Dakoulas, P. and Gazetas, G., (1986b) "Seismic Shear Strains and Seismic Coefficients in Dams and Embankments," *Journal of Soil Dynamics and Earthquake Engineering*, Vol. 5, pp. 75-83.

Dakoulas, P. and Gazetas, G., (1987) "Vibration Characteristics of Dams in Narrow Canyons," *Journal of Geotechnical Engineering ASCE*, Vol. 113, No. 8.

Gazetas, G. (1987) "Seismic Response of Earth Dams: Some Recent Developments," *Journal of Soil Dynamics and Earthquake Engineering* 6(1), pp. 2 - 47.

Gazetas, G., (1982) "Shear Vibrations of Vertically Inhomogeneous Earth Dams", *International Journal for Numerical and Analytical Methods in Geomechanics*, 6 (2), pp. 216 - 241.

Hashmi, H. (1989) "Response of Earth Dams in Canyons Subjected to Asynchronous Base Excitation", M.S. thesis, Rice University, Houston, Texas.

Makdisi, F. I., Kagawa, T. & Seed, H. B., (1982) "Seismic Response of Earth Dams in Triangular Canyons," *Journal of Geotechnical Engineering Division, ASCE*, 108, GT10, pp 1328-1337.

Martinez, B. & Bielak, J., (1980) "On the Three-Dimensional Seismic Response of the Earth Structures," *Proc. 7th World Conference on Earthquake Engineering*, Vol. 8, Istanbul, pp. 523-528.

Mejia, L. H. & Seed, H. B., and Lysmer, J., (1982) "Dynamic Analysis of Earth Dams in Three Dimensions", *Journal of Geotechnical Engineering Division, ASCE*, 108, GT12, pp. 1586-1604.

Mejia, L. H. & Seed, H. B., (1983) "Comparison of 2-D and 3-Dynamic Analyses of Earth Dams" *Journal of Geotechnical Engineering Division, ASCE*, 109,GT11, pp.1383 -1398.

Ohmachi, T., (1981) "Analysis of Dynamic Shear Strain Distributed 3-Dimensional Earth Dam Models" *Proc. Int. Conf. on Recent Advances in Geotech. Earthq. Engrg. and Soil Dyn.*, Vol. 1, St. Louis, pp.459-464.

Roesset, J., (1977) "Soil Amplification of Earthquakes". *Numerical Methods in Geotechnical Engineering*, Edited by Desai and Christiano, Mc-Graw Hill.

Trifunac, M. D., (1973) "Scattering of Plane SH Waves by a Semi-Cylindrical Canyon," *Int. Journal of Earthquake Engineering and Structural Dynamics*, 1, 3, 267-281.

Trifunac, M. D., (1977) "Surface Motion of a Semi-cylindrical Alluvial Valley for Incident Plane SH Waves", *Bulletin of the Seismological Society of America*, Vol. 61, No. 6, pp. 1755-1770.

Wong, H. L., Trifunac, M. D., (1974) "Surface Motion of a Semi-Elliptical Alluvial Valley for Incident Plane SH Waves," *Bulletin of the Seismological Society of America*, Vol. 64, pp. 1389 - 1408.